Calculation of displacement damage cross-section for charged particles at energies up to 100 GeV

Wen Yin[*,a,b], A.Yu. Konobeyev[b], D. Leichtle[b], Liangzhi Cao[a]

[a] School of Nuclear Science and Technology, Xi'an Jiaotong University, Xi'an, Shaanxi, 710049, China

[b] Institute for Neutron Physics and Reactor Technology, Karlsruhe Institute of Technology, Eggenstein-Leopoldshafen, 76344, Germany

Abstract: Accurate prediction of displacement damage is essential for the safety of nuclear materials irradiated by neutrons, gammas and charged particles. Displacement damage cross-sections are used for the calculation of displacement damage rate. With the development of accelerator facilities and spallation neutron sources, displacement damage rate calculations in these facilities require the availability of displacement damage cross-sections for charged particles. In the present work, new arc-dpa model parameters were obtained for aluminum, iron, copper and tungsten. The displacement damage cross-sections for protons, deuterons, and alpha-particles at energies up to 100 GeV are calculated using the standard NRT and the arc-dpa model with improved parameters for these materials. Calculated displacement damage cross-sections for charged particles calculated using the arc-dpa model with new parameters agree well with available experimental data.

Keyword: displacement damage cross-section; charged particle; arc-dpa model; NRT model; radiation damage

1. Introduction

A reliable estimation of displacement damage of materials irradiated by charged particles is an essential part of the work for the safety of the spallation neutron sources, light-ion facilities and proton facilities. Over the past few decades, a number of related facilities have been in operation. The major spallation neutron sources are the Spallation Neutron Source [1], Japan Proton Accelerator Research Complex (J-PARC) [2], ISIS Neutron and Muon Source [3], China Spallation Neutron Source [4], etc. Proton facilities and light-ion facilities such as AIFIRA (Applications

* Corresponding author.
E-mail address: wen_yin2022@126.com (Wen Yin).

Interdisciplinaires des Faisceaux d'ions en Région Aquitaine) [5], Proton Irradiation Facility at PSI (Paul Scherrer Institut) [6], BISOL (Beijing Isotope-Separation-On-Line Neutron-Rich Beam Facility) [7] and others are intensively used in scientific research area. Recently, new high-power spallation neutron sources and ion facilities are coming up, such as the European Spallation Source [8], the Facility for Rare Isotope Beams [9], and the International Fusion Materials Irradiation Facility [10]. Proton, deuteron, alpha-particle and heavy charged particles are part of radiation sources in these facilities besides neutrons. The power of the facilities is increasing along the time to meet the needs of users and researches. The energies of the particles range from eV to GeV/nucleon. Accurate calculation of the displacement damage cross-section for charged particles is a vital task for reliable estimation of displacement damage rate of materials in spallation neutron sources, proton facilities and light-ion facilities.

In the 1960s, the research activities [11, 12] involving proton displacement damage calculations were performed for silicon and germanium. They have used immature displacement damage models and considered the displacement damage caused by Coulomb scattering only [11]. Apart from Coulomb scattering, nuclear elastic scattering contributes to displacement damage at the proton energies larger than 10 MeV and nonelastic collisions become more important with the increasing of proton incident energy [13]. Considering the nuclear elastic scattering, Edward et al. [13] have calculated the energy dependence of proton-induced displacement damage in silicon and introduced the displacement damage produced by nonelastic collision though it has not been included in the final results. In the 1970s, the displacement models had become increasingly sophisticated and the Norgett−Robinson−Torrens (NRT) model [14] became the "standard" displacement damage model used for different applications. Earlier studies for charged particles displacement damage were usually applied in semiconductor industry, where primary particles energies were not very high. With the development of spallation neutron sources, proton facilities and light-ion facilities, the energy of charged particles increased significantly. The authors [15] have calculated the displacement damage cross-sections for tantalum and tungsten irradiated with protons at energies up to 1 GeV, where both elastic and nonelastic scattering were considered and NRT model was used. In the following research, the authors [16,17] increased the maximum incident energy and expanded the isotopes for displacement damage cross-sections, and also improved the precision using the corrected displaced atom number which was calculated based on the results of

molecular dynamics (MD) and binary collision approximation (BCA) simulations. Recently Iwamoto and coauthors calculated displacement damage cross-sections using the PHITS (Particle and Heavy Ion Transport code System) code [18] for charged particles [19]. A physically realistic damage model, named arc-dpa (athermal recombination corrected dpa) model, was proposed by Nordlund et al. in 2015. After the proposal of the arc-dpa model [20], this model and combination of arc-dpa and BCA model were adopted to describe the number of displaced atoms [21] in the proton displacement damage cross-section calculation. Using experimental data as the reference, the proton displacement damage cross-sections were substantially improved, but many problems remain [21]. For example, the proton displacement damage cross-sections for copper are far away from the experimental data.

Up to now, there is no systematic calculation for the deuteron and alpha-particle displacement damage cross-sections. Such calculations are important for reliable estimation of radiation damage rate in deuteron facilities, alpha-particle facilities, etc.

In the present work, the calculation of displacement damage cross-section for proton, deuteron, and alpha-particle was performed for aluminum, iron, copper, and tungsten at incident energies up to 100 GeV. Both arc-dpa and NRT models were used for the calculation. The new arc-dpa model parameters were obtained using available experimental proton displacement damage cross-sections. In the calculation of elastic displacement damage cross-section, the LNS (Lindhard-Nielsen-Scharff) formula [22] was used for energies below several MeV; In the intermediate energy range, above several MeV and below 50 - 250 MeV, the calculations were performed using the ECIS (Equations Couplées en Itérations Séquentielles) code [23] applying different optical model potentials; At primary particle energies above 50 – 250 MeV, the relativistic Rutherford formula was used. In the calculation of the nonelastic contribution to the displacement damage cross-section, four different nuclear models as implemented in the MCNP6 (Monte Carlo N-Particle) [24], PHITS [18] and CASCADE [25] codes were applied.

The methods of the displacement damage cross-section calculation for charged particles and new arc-dpa model parameters are described in Section 2. In Section 3, the results of displacement damage cross-sections for charged particles are presented and discussed.

2. Methodology

The total displacement damage cross-section is the sum of the cross-section by elastic

scattering of primary particles on atoms $\sigma_{d,el}$ and the cross-section by nonelastic interactions of particles with nuclei $\sigma_{d,non}$. The general formula used to calculate displacement damage cross-section is written as follows:

$$\sigma_d(E)=\sum_i \int_{E_d}^{T_i^{\max}} \nu(T_i)\frac{\mathrm{d}\sigma(E,T_i)}{\mathrm{d}T_i}\mathrm{d}T_i \tag{1}$$

where E is the incident charged particles energy; $\mathrm{d}\sigma(E,T_i)/\mathrm{d}T_i$ is the recoil energy distribution of *i*-th nuclear interaction. $T_i^{\max}$ is the maximum energy of recoil atom produced in the *i*-th nuclear interaction; E_d is the threshold displacement energy of target material; $\nu(T_i)$ is the number of displaced atoms.

In this paper the arc-dpa and NRT model are used to obtain the number of displaced atoms. The calculations of recoil energy distributions in nuclear interactions and the number of displaced atoms are discussed below.

2.1 Calculation method of recoil energy distributions in nuclear interaction

2.1.1. Elastic scattering of charged particles

The correct description of the recoil energy distribution in the charged particle elastic interaction concerns the considerations of the screened Coulomb scattering in material, the nuclear scattering and their interference. Considering the importance of different scattering processes in different energy range, different methods or formulas are used in three energy ranges.

For the charged particles energy below several MeV, the screening effect plays an important role in the particle scattering on atoms. In this case the recoil energy distribution can be estimated using the LNS formula [22] as follows:

$$\mathrm{d}\sigma(E,T)=\pi a_{ij}^2\frac{f(t^{1/2})}{2t^{3/2}}dt \tag{2}$$

where $f(t^{1/2})$ is the scattering function [26]; *E* and *T* are the incident particle energy and recoil energy, respectively; a_{ij} is the screening length; For the Lindhard screening length, it is written as follows:

$$a_{ij} = \frac{0.8853 a_0}{\left(Z_i^{2/3} + Z_j^{2/3}\right)^{1/2}} \tag{3}$$

and t is the reduced energy which is equal to:

$$t = \frac{TEM_j}{M_i}\left(\frac{a_{ij}}{2Z_i Z_j e^2}\right)^2 \tag{4}$$

where a_0 is the Bohr radius; Z_i and Z_j are the atomic number of incident particle and recoil, respectively; M_i and M_j are the atomic mass of incident particle and recoil, respectively; e is the elementary charge.

The scattering function $f(t^{1/2})$ uses a common analytical approximation proposed by Winterbon et al. [27]:

$$f\left(t^{1/2}\right) = \lambda t^{1/2-m}\left[1+\left(2\lambda t^{1-m}\right)^q\right]^{-1/q} \tag{5}$$

where λ, m and q are fitting parameters. Many sets of fitting parameters corresponding to different screening functions are collected in the book [26]. The authors [16] compared the displacement damage cross-sections calculated using different screening functions. The differences between different scattering functions are acceptable. The Thomas-Fermi version [27] of the scattering function is adopted in this paper. λ, m and q are 1.309, 1/3 and 2/3, respectively.

The contribution of nuclear elastic scattering in the recoil energy distribution becomes significant at energies above ~5MeV, where screening effect tends to be negligible. At this energy range the optical model can be used for elastic displacement damage cross-section calculations.

Table 1 summaries the commonly used global optical model potentials for protons, deuterons and alpha-particles. As in the Ref [21], the calculations were performed using the optical model with parameters of Koning and Delaroche [28] at the energies between 5 and 50 MeV, and Madland's parameters [29] between 50 and 250 MeV. For incident deuteron, three global optical model potentials (An-Cai [30], Han-Shi-Shen [31] and Bojowald-Machner-Nann [32] potential) are available for recoil energy distribution calculations. Because the An-Cai potential [30] has wider energy and isotope range in contrast to other potentials, the An-Cai potential was used for the recoil energy distribution calculation for the deuteron elastic scattering in the middle energy range, commonly from several MeV to several hundred MeV. Avrigeanu-Hodgson-Avrigeanu potential [33]

was used in the recoil energy distribution calculation for the alpha-particle elastic scattering. The numerical calculations were performed using the ECIS06 code [23] based on these potentials.

At high incident energies, beyond the applicability of optical model potentials, the relativistic formula [38] is used up to 100 GeV for recoil energy distribution calculation for elastic scattering. Because of several typos of the Refs. [38,39], the correct relativistic formulate is repeated here:

$$d\sigma(E,T) = \frac{\pi b^2 T_{\max}}{4\gamma^2}\left[1-\beta^2\frac{T}{T_{\max}} + \pi\alpha\beta\left(\left(\frac{T}{T_{\max}}\right)^{1/2} - \frac{T}{T_{\max}}\right)\right]\frac{dT}{T^2} \quad (6)$$

where $b = \frac{2zZe^2}{mc^2\beta^2}$; $\beta = \frac{v}{c} = \sqrt{1-\left(\frac{mc^2}{mc^2+E}\right)^2}$; $\gamma = \frac{1}{\sqrt{1-\beta^2}}$; $\alpha = \frac{Ze^2}{\hbar c} = \frac{Z}{137.036}$;

$T_{\max} = \frac{2E(E+2mc^2)}{(1-\frac{m}{M})^2 Mc^2 + 2E}$. In Eq. (6), v, m, z and E are the charged particle velocity, mass, charge, and energy, respectively. M and Z refer to the mass and charge of target material. T is the energy transferred to recoil atom. $\hbar$, c and e refer to the reduced Planck constant, speed of light and elementary charge.

The elastic displacement damage cross-sections calculated using different optical model potentials, LNS and relativistic formulas were compared in this work. Figs.1 and 2 show the results of iron irradiated by deuteron and alpha-particles, respectively. The deuteron elastic displacement damage cross-sections calculated using different optical model potentials are close. There is obvious difference between optical model and LNS formula calculations at the energies about 5 MeV. It means that nuclear elastic scattering plays an important role at the energies above about 5 MeV. The elastic displacement damage cross-sections are close to that calculated by relativistic formula above 100 MeV and it demonstrates that the relativistic formula can be applied in elastic displacement damage cross-section calculation at high energy even though it does not consider the nuclear elastic scattering. The similar conclusion can also be obtained from the comparison of cross-sections shown in Fig.2. The differences of elastic displacement damage cross-sections for alpha-particle using several optical model potentials are rather small and the results obtained using optical model agree well with the cross-sections calculated using LNS and relativistic formulas.

2.1.2. Nonelastic interaction of charged particles

With the increasing of incident energy of charged particles, elastic displacement damage cross-section decreases and nonelastic interactions with atoms become more important. To calculate the nonelastic displacement damage cross-section, various nuclear models implemented in the MCNP6 [24], CASCADE [25], and PHITS [18] codes were used to obtain the recoil energy distributions. In Table 2, the intra-nuclear cascade (INC) models, pre-equilibrium models, equilibrium models, projectiles and upper energy limitations for these models are summarized. Considering the upper energy limitation of incident particle and the type of projectiles, four nuclear models, INCL4.2 combined with ABLA [43] from MCNP6, LAQGSM03.03 from MCNP6, INCL4.6 [44] combined with JAMQMD [18] from PHITS, and CASCADE, were used for the displacement damage cross-section calculation up to 100 GeV.

2.2 Calculation models for the number of displaced atoms

Besides the calculation of recoil energy distributions in nuclear interactions, the calculation of displaced atoms number $\nu(T_i)$ in Eq. (1) is another part of displacement damage cross-section evaluation. Arc-dpa and NRT models used to obtain displaced atoms number are described below.

2.2.1. NRT model

According to the NRT model, the number of displaced atoms can be calculated as:

$$\nu(E_a)=\begin{cases}0, & 0<E_a<E_d\\ 1, & E_d<E_a<\dfrac{2E_d}{0.8}\\ \dfrac{0.8E_a}{2E_d}, & \dfrac{2E_d}{0.8}<E_a<\infty\end{cases} \tag{7}$$

where $\nu(E_a)$ is the number of displaced atoms. E_a is the Lindhard's damage energy [45]. E_d is the threshold displacement energy taken equal to 27, 40, 33, and 70 eV for Al, Fe, Cu and W, respectively [20].

2.2.2. Arc-dpa model

Observed overestimations of the number of displaced atoms promote the proposal for new displacement damage function model [46-47]. Nordlund et al. proposed a new calculation model for displaced atoms number, arc-dpa model [20], by considering results of MD simulations. According to Ref. [20], the formula for arc-dpa model is written as follows:

$$\nu(E_a)=\begin{cases} 0, & 0<E_a<E_d \\ 1, & E_d<E_a<\dfrac{2E_d}{0.8} \\ \dfrac{0.8E_a}{2E_d}\xi(E_a), & \dfrac{2E_d}{0.8}<E_a<\infty \end{cases} \tag{8}$$

where $\xi(E_a)$ is the efficiency function given by:

$$\xi(E_a)=\frac{1-c}{(2E_d/0.8)^b}E_a^b+c \tag{9}$$

where *b* and *c* are model parameters to be determined from MD simulations or experimental data. The following *b*, and *c* values are the original arc-dpa model parameters, correspondingly, for Al: −0.82, 0.443 [21], for Fe: −0.568, 0.286 [20], for Cu: −0.68, 0.16 [20], and for W: −0.56, 0.12 [20]. These original arc-dpa model parameters are from the fitting based on MD simulation data.

2.2.3. Obtaining of new arc-dpa model parameters

In recent years, a number of measurements were performed for proton displacement damage cross-section [48-53]. New arc-dpa model parameters were obtained using measured displacement damage cross-sections of incident protons (Table 3). Because the arc-dpa model parameters depend on the material types but not incident particle types, the parameters were applied for cross-section calculation for not only incident protons, but also deuterons and alpha-particles.

For iron and copper, the number of experimental data in Table 3 is sufficient for obtaining the arc-dpa model parameters. But there is only one measured proton displacement damage cross-section for aluminum and three for tungsten. So, the data derived from electron, light ion, self-ion or neutron experimental data by Jung [54] are also used for the model parameters fitting for aluminum and tungsten. For those displacement damage cross-sections in Table 3 without uncertainties, 30% is adopted as their uncertainties. The experimental displacement damage cross-sections σ_d^e in Table 3 were obtained by:

$$\sigma_d^e=\frac{1}{\rho_F}\frac{\Delta\rho}{\Delta\phi} \tag{10}$$

where $\Delta\rho/\Delta\phi$ the damage rate which is measured in experiments; ρ_F is the Frenkel pair resistivity taken equal to 3.7, 24.6, 2.2 and 27 $\mu\Omega\cdot m$ for Al, Fe, Cu and W, respectively [55].

The arc-dpa model parameter *b* was selected from -1.0 to -0.01 and *c* was selected from 0.01 to 1.0 according to their possible physical limitation. In this work, the parameters *b* and *c* are divided into 100 equal parts, respectively, and thus 10000 sets of parameters are obtained. And then proton displacement damage cross-sections are calculated using the methods described in Sec. 2 using every sets of parameters. Finally, all 10000 sets of calculated proton displacement damage cross-sections are compared with the experimental data from Table 3 and Jung's paper [54] using the deviation factor [56]:

$$H = \left(\sum_{1}^{N} \left(\frac{\sigma_i^{\exp} - \sigma_i^{calc}}{\Delta\sigma_i^{\exp}} \right) / N \right)^{0.5} \tag{11}$$

where N is the number of experimental data, $\sigma_i^{\exp}$ and σ_i^{calc} are the experimental and calculated displacement damage cross-section and $\Delta\sigma_i^{\exp}$ is the uncertainty of the experimental data.

The model parameters corresponding to the smallest *H* value are the final new arc-dpa model parameters. Table 4 summaries the new parameters for Al, Fe, Cu and W based on four different nuclear models. Various nuclear models have corresponding arc-dpa model parameters. The parameters should be used for nuclear models correspondingly in all charged particles displacement damage cross-section calculation.

3. Results and discussion

3.1. Proton displacement damage cross-section

Proton displacement damage cross-sections were calculated using new arc-dpa model parameters. Figs. 3 – 6 show the new proton displacement damage cross-sections, results of previous calculations and experimental data. The displacement damage cross-sections obtained by using four different nuclear models (INCL4.2 combined with ABLA, LAQGSM03.03, INCL4.6 combined with JAMQMD, CASCADE) and using the arc-dpa and NRT model are also shown in these figures.

The use of different nuclear models leads to the bias of the displacement damage cross-sections at high energies where the nonelastic interactions have dominant contributions to displacement damage cross-sections. The final cross-sections are obtained by averaging all results based on different nuclear models. It means practically, that there is no preference of any model, such that a simple average might be a more reliable result. The results obtained using all four nuclear models were used for averaging below 1 GeV; considering the upper energy limitations of different nuclear

model, the cross-sections calculated using all nuclear models except CASCADE were averaged between 1 GeV and 3 GeV; only the results calculated using MCNP based on LAQGSM03.03 and PHITS were used between 3 GeV and 100 GeV.

Although arc-dpa model is more accurate than NRT model because its model parameters were obtained using MD simulation data, its results still cannot agree well with the experimental data at higher incident energies. Compared with the arc-dpa model using original model parameters, arc-dpa model coupled with BCA model [21] improved the agreement with the experimental data. The improved results show better performance for a number of nuclides, but some displacement damage cross-sections also can't agree well with the experimental data, especially for Cu [21]. The improved proton displacement damage cross-sections in this work agree better with the experimental data than all previous results.

The displacement cross section decreases at high energies for light target nuclides, such as Al, Fe and Cu. But it increases first and decreases later for heavy nuclide tungsten. This rule of change is similar to the change in nonelastic cross-section. The reason is that when the recoil energy exceeds about 1 MeV, the damage energy saturates as the recoil energy increases because the energy lost in the cascade due to electronic excitation is subtracted. The same conclusion also applies to incident deuteron and alpha-particle.

The uncertainties of the displacement damage cross-sections are due to the uncertainties of arc-dpa model parameters, nuclear models' predictions, and the threshold displacement energy. It is a complicated task to calculate these terms of uncertainties completely. Only the uncertainty propagated from nuclear models' predictions is calculated based on different results obtained by different nuclear models in this paper. The uncertainty is equal to the standard deviation of different nuclear models' results. The maximum uncertainty of improved proton displacement damage cross-sections propagated from nuclear models' predictions is about 17% for aluminum. For other nuclides, the uncertainty is less than 10%.

3.2. Deuteron displacement damage cross-section

Fig. 7 shows the typical contributions of elastic and nonelastic processes to the deuteron displacement damage cross-sections. The contribution of elastic scattering dominates at relatively low incident energies below 10 MeV/nucleon, and with increasing energy it is inferior to nonelastic

processes, which become dominant at energies above 50 MeV/nucleon.

In this work, the averaging strategy for proton is also used for deuteron. Figs. 8 - 11 show the deuteron displacement damage cross-section calculated using arc-dpa model with new model parameters and NRT model. Experimental data are taken from Jung [54]. The calculated deuteron displacement damage cross-sections agree well with the experimental data. For iron and copper, the uncertainties are less than 20%. The maximum uncertainty of deuteron displacement damage cross-sections propagated from nuclear models' predictions for aluminum and tungsten are about 30% and 38%, correspondingly.

3.3. Alpha-particle displacement damage cross-section

Fig. 12 shows the typical contributions of elastic and nonelastic processes to the alpha-particle displacement damage cross-sections. The contribution of elastic scattering dominates at alpha-particle energies below 25 MeV/nucleon, and with the energy increasing nonelastic processes become dominant at energies above 250 MeV/nucleon.

The PHITS code doesn't have the ability to calculate alpha-particle displacement damage cross-sections calculation directly until now. In alpha-particle displacement damage cross-section calculation, the results obtained using all nuclear models except PHITS are averaged below 250 MeV/nucleon; the results obtained from MCNP calculation using two models were averaged between 250 MeV/nucleon and 750 MeV/nucleon; alpha-particle displacement damage cross-sections between 750 MeV/nucleon and 25 GeV/nucleon were calculated using LAQGSM model.

Figs. 13 - 16 show the alpha-particle displacement damage cross-section calculated using arc-dpa model with new model parameters and NRT model. Experimental data are from Ref [54]. Similar to proton and deuteron displacement damage cross-sections, the alpha-particle displacement damage cross-sections also agree well with experimental data. The maximum uncertainty of alpha-particle displacement damage cross-sections propagated from nuclear models' predictions is about 19% for tungsten and the uncertainty is less than 10% for other nuclides.

3.4. Recommendation for the use of evaluated displacement damage cross-section

Proton, deuteron and alpha-particle displacement damage cross-sections for Al, Fe, Cu and W

were evaluated using the arc-dpa model with model parameters obtained in this paper and NRT model. The NRT model is used still as an international standard for displacement damage calculations. However, calculated cross-sections based on arc-dpa model with improved model parameters are more physically realistic and agree better with experimental data and can be recommended for displacement damage calculations.

Displacement damage cross-sections obtained using the arc-dpa model with improved parameters and NRT model were recorded using the ENDF-6 format, which can be processed with the NJOY code. The obtained displacement damage cross-sections are available in Ref. [57]. It is convenient for radiation damage rate calculations in the future.

4. Conclusions

Proton, deuteron and alpha-particle displacement damage cross-sections for Al, Fe, Cu, and W were obtained at incident particle energies up to 100 GeV using the arc-dpa model with improved model parameters and NRT model. New arc-dpa model parameters were obtained using available experimental displacement damage cross-sections for incident protons (Table 4). The obtained defect generation efficiency for Al, Fe, Cu, and W can also be used for displacement damage cross-section calculation for any incident particles. The discussed calculation method for displacement damage cross-section can also be used for the calculation of displacement damage cross-sections for all other materials using arc-dpa model with original arc-dpa model parameters or NRT model.

The obtained displacement damage cross-sections are available in Ref. [57]. The displacement damage cross-sections calculated using arc-dpa model with new model parameters show better performance than arc-dpa model with original model parameters. It demonstrates that the obtained displacement damage cross-sections can be recommended for use in calculation of improved radiation damage rates for the investigated materials.

Acknowledgements

This research was financially supported by China Scholarship Council (No. 202106280113).

References

[1] T. A. Gabriel, J. R. Haines, T. J. McManamy, Overview of the Spallation Neutron Source

(SNS) with emphasis on target systems. J. Nucl. Mater. 318 (2003), 1-13.

[2] S. Nagamiya, Introduction to J-PARC. Prog. Theor. Exp. Phys. 2012, 02B001.

[3] D. J. S. Findlay, ISIS-pulsed neutron and muon source. In 2007 IEEE Particle Accelerator Conference (PAC). IEEE, 2007, 695-699.

[4] J. Wei, S. Fu, J. Tang, et al., China Spallation Neutron Source - an overview of application prospects. Chin. Phys. C, 33(2009), 1033-1042.

[5] P. Barberet, J. Jouve, S. Sorieul, et al., AIFIRA: a light ion beam facility for ion beam analysis and irradiation. Eur. Phys. J. Plus, 136(2021), 1-10.

[6] W. Hajdas, L. Adams, B. Nickson, et al., The proton irradiation facility at the Paul Scherrer institute. Nucl. Instr. Meth. B, 113(1996), 54-58.

[7] S. X. Peng, F. Zhu, Z. Wang, et al., The deuteron accelerator preliminary design for BISOL. Nucl. Instr. Meth. B, 376(2016), 420-424.

[8] M. Lindroos, S. Bousson, R. Calaga, et al., The European spallation source. Nucl. Instr. Meth. B, 269(2011), 3258-3260.

[9] M. Thoennessen, Plans for the facility for rare isotope beams. Nucl. Phys. A, 834(2010), 688-693.

[10] K. Ehrlich, A. Möslang, IFMIF–An international fusion materials irradiation facility. Nucl. Instr. Meth. B, 139(1998), 72-81.

[11] G.W. Simon, J. M. Denny, R. G. Downing, Energy dependence of proton damage in silicon. Phys. Rev., 129(1963), 2454–2459.

[12] J. R. Bilinski, E. H. Brooks, U. Cocca, et al., Proton-neutron damage equivalence in Si and Ge semiconductors. IEEE Trans. Nucl. Sci., 10(1963), 71–86.

[13] E. A. Burke, Energy dependence of proton-induced displacement damage in silicon. IEEE Trans. Nucl. Sci., 33(1987), 1276-1281.

[14] M. J. Norgett, M. T. Robinson, I. M. Torrens, A proposed method of calculating displacement dose rates. Nucl. Eng. Des., 33(1975), 50-54.

[15] C. H. M. Broeders, A. Yu. Konobeyev, Displacement cross-sections for tantalum and tungsten irradiated with protons at energies up to 1 GeV. J. Nucl. Mater., 336(2005), 201-209.

[16] A. Yu. Konobeyev, C. H. M. Broeders, U., Fischer, Improved displacement cross sections

for structural materials irradiated with intermediate and high energy protons. In Proc. 8th International Topical Meeting on the Nuclear Applications of Accelerator Technology (AccApp'07), 2007, 241-248.

[17] A. Yu. Konobeev, U. Fischer, DPA and gas production in intermediate and high energy particle interactions with accelerator components. HB2014 proceedings, 2015, THO4AB02.

[18] T. Sato, Y. Iwamoto, S. Hashimoto, et al., Features of particle and heavy ion transport code system (PHITS) version 3.02. J. Nucl. Sci. Tech., 55(2018), 684-690.

[19] Y. Iwamoto, K. Niita, T. Sawai, et al., Displacement damage calculations in PHITS for copper irradiated with charged particles and neutrons. Nucl. Instr. Meth. B, 303(2013), 120-124.

[20] K. Nordlund, S. J. Zinkle, A. E. Sand, et al., Improving atomic displacement and replacement calculations with physically realistic damage models. Nat. Commun., 9(2018), 1-8.

[21] A. Yu. Konobeyev, U. Fischer, S. P. Simakov, Improved atomic displacement cross-sections for proton irradiation of aluminium, iron, copper, and tungsten at energies up to 10 GeV. Nucl. Instr. Meth. B, 431(2018), 55-58.

[22] J. Lindhard, V. Nielsen, M. Scharff, Approximation method in classical scattering by screened coulomb fields (Notes on Atomic Collisions, I), Mat. Fys. Medd. Dan. Vid. Selsk. 36(1968), 10.

[23] J. Raynal, Notes on ECIS94. CEA Saclay report CEA-N-2772, 1994.

[24] J. T. Goorley, M. R. James, T. E. Booth, et al., Initial MCNP6 release overview-MCNP6 version 1.0. Los Alamos National Lab.(LANL), Los Alamos, NM (United States), No. LA-UR-13-22934, 2013.

[25] V. S. Barashenkov, Monte Carlo simulation of ionization and nuclear processes initiated by hadron and ion beams in media. Comput. Phys. Commun., 126(2000), 28-31.

[26] M. Nastasi, N. Michael, J. Mayer, et al., Ion-solid interactions: fundamentals and applications. 1996, Cambridge University Press.

[27] K.B. Winterbon, P. Sigmund, J.B.K. Sanders, Spatial distribution of energy deposited by atomic particles in elastic collisions, Mat. Fys. Medd. Dan. Vid. Selsk. 37(1970), 14.

[28] A. J. Koning, J. P. Delaroche, Local and global nucleon optical models from 1 keV to 200 MeV. Nucl. Phys. A, 713(2003). 231-310.

[29] D.G. Madland, OECD/NEA Spec. Mtg. Nucleon-Nucleus. Opt. Mod. to 200MeV, Paris, 1997, p. 129.

[30] H. An, C. Cai, Global deuteron optical model potential for the energy range up to 183 MeV. Phys. Rev. C, 73(2006), 054605.

[31] Y. Han, Y. Shi, Q. Shen, Deuteron global optical model potential for energies up to 200 MeV. Phys. Rev. C, 74(2006), 044615.

[32] J. Bojowald, H. Machner, H. Nann, et al., Elastic deuteron scattering and optical model parameters at energies up to 100 MeV. Phys. Rev. C, 38(1988), 1153.

[33] V. Avrigeanu, P. E. Hodgson, M. Avrigeanu, Global optical potentials for emitted alpha particles. Phys. Rev. C, 49(1994), 2136.

[34] V. Avrigeanu, M. Avrigeanu, C. Mănăilescu, Further explorations of the α-particle optical model potential at low energies for the mass range A≈ 45–209. Phys. Rev. C, 90(2014), 044612.

[35] https://www-nds.iaea.org/RIPL-3/

[36] A. J. Koning, D. Rochman, J. C. Sublet, et al., TENDL: complete nuclear data library for innovative nuclear science and technology. Nucl. Data Sheets, 155 (2019), 1-55.

[37] A. J. Koning, S. Hilaire, M. C. Duijvestijn, TALYS-1.0. In International Conference on Nuclear Data for Science and Technology. EDP Sciences, 2007, 211-214.

[38] I. Jun, Effects of secondary particles on the total dose and the displacement damage in space proton environments. IEEE Trans. Nucl. Sci., 48(2001), 162-175.

[39] E. A. Burke, Energy dependence of proton-induced displacement damage in silicon. IEEE Trans. Nucl. Sci., 33(1986), 1276-1281.

[40] Y. Yariv, Z. Fraenkel, Intranuclear cascade calculation of high-energy heavy-ion interactions. Phys. Rev. C, 20(1979), 2227.

[41] A. Boudard, J. Cugnon, S. Leray, et al., Intranuclear cascade model for a comprehensive description of spallation reaction data. Phys. Rev. C, 66(2002), 044615.

[42] S. G. Mashnik, K. K. Gudima, N. V. Mokhov, et al., LAQGSM03. 03 Upgrade and its Validation. 2007.

[43] J. J. Gaimard, K. H. Schmidt, A reexamination of the abrasion-ablation model for the description of the nuclear fragmentation reaction. Nucl. Phys. A, 531(1991), 709-745.

[44] A. Boudard, J. Cugnon, J. C. David, et al., New potentialities of the Liège intranuclear cascade model for reactions induced by nucleons and light charged particles. Phys. Rev. C, 87(2013), 014606.

[45] J. Lindhard, V. Nielsen, P. V. Thomsen, Integral equations governing radiation effects. Mat. Fys. Medd. Dan. Vid. Selsk., 33(1963), 1-42.

[46] R. S. Averback, R. Benedek, K. L. Merkle, Ion-irradiation studies of the damage function of copper and silver. Phys. Rev. B, 18(1978), 4156.

[47] S. J. Zinkle, B. N. Singh, Analysis of displacement damage and defect production under cascade damage conditions. J. Nucl. Mater., 199(1993),173-191.

[48] H. Matsuda, S. I. Meigo, Y. Iwamoto, et al., Measurement of displacement cross-sections of copper and iron for proton with kinetic energies in the range 0.4–3 GeV. J. Nucl. Sci. Tech., 57(2020), 1141-1151.

[49] Y. Iwamoto, M. Yoshida, H. Matsuda, et al., Measurements of displacement cross section of tungsten under 389-MeV proton irradiation and thermal damage recovery. In Materials Science Forum, Trans Tech Publications Ltd. 1024(2021), 95-101.

[50] Y. Iwamoto, M. Yoshida, T. Yoshiie, et al., Measurement of displacement cross sections of aluminum and copper at 5 K by using 200 MeV protons. J. Nucl. Mater., 508 (2018), 195-202.

[51] Y. Iwamoto, T. Yoshiie, M. Yoshida, T., Nakamoto, et al., Measurement of the displacement cross-section of copper irradiated with 125 MeV protons at 12 K. J. Nucl. Sci. Tech., 458(2015), 369-375.

[52] Y. Iwamoto, M. Yoshida, H. Matsuda, et al., Measurement of defect-induced electrical resistivity change of tungsten wire at cryogenic temperature using high-energy proton irradiation. In Proceedings of the 14th International Workshop on Spallation Materials Technology, 2020, 061003.

[53] G. A. Greene, C. L. Snead Jr, C. C. Finfrock, et al., Direct measurements of displacement cross sections in copper and tungsten under irradiation by 1.1-GeV and 1.94-GeV Protons at 4.7 K. In Proc. Sixth International Meeting on Nuclear Applications of Accelerator

Technology (AccApp'03), San Diego, 2003, 881-892.

[54] P. Jung, Atomic displacement functions of cubic metals. J. Nucl. Mater. 117(1983), 70-77.

[55] C. H. M. Broeders, A. Yu. Konobeyev, Defect production efficiency in metals under neutron irradiation. J. Nucl. Mater., 328(2004), 197-214.

[56] A. Yu. Konobeyev, U. Fischer, A. J. Koning, et al., What can we expect from the use of nuclear models implemented in MCNPX at projectile energies below 150 MeV? Detailed comparison with experimental data. J. Korean Phys. Soc., 59(2011), 927-930.

[57] W. Yin. https://bit.ly/3PxuS8n.

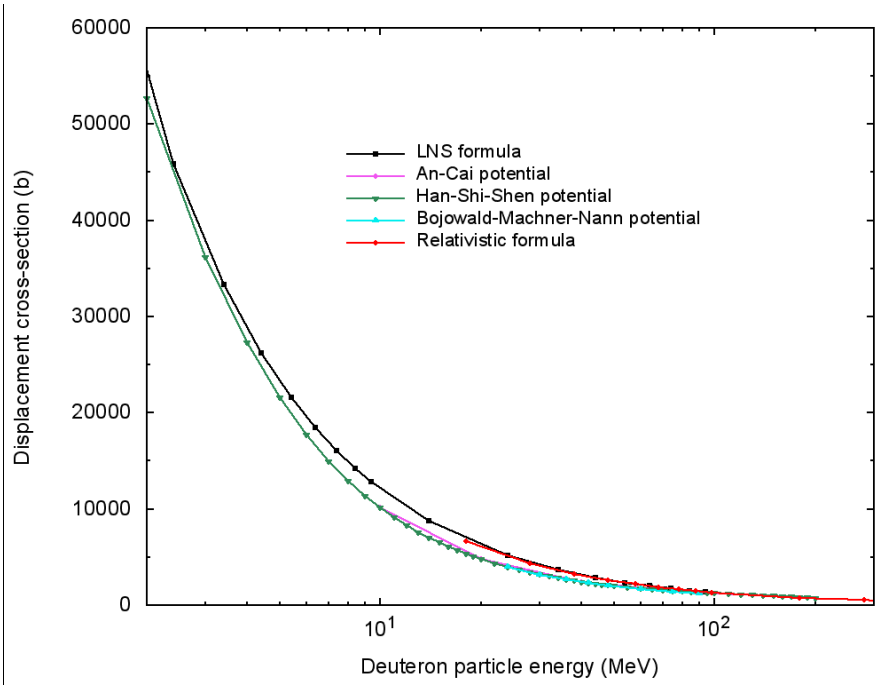

Fig. 1 Deuteron elastic displacement damage cross-section of Fe in different energy ranges

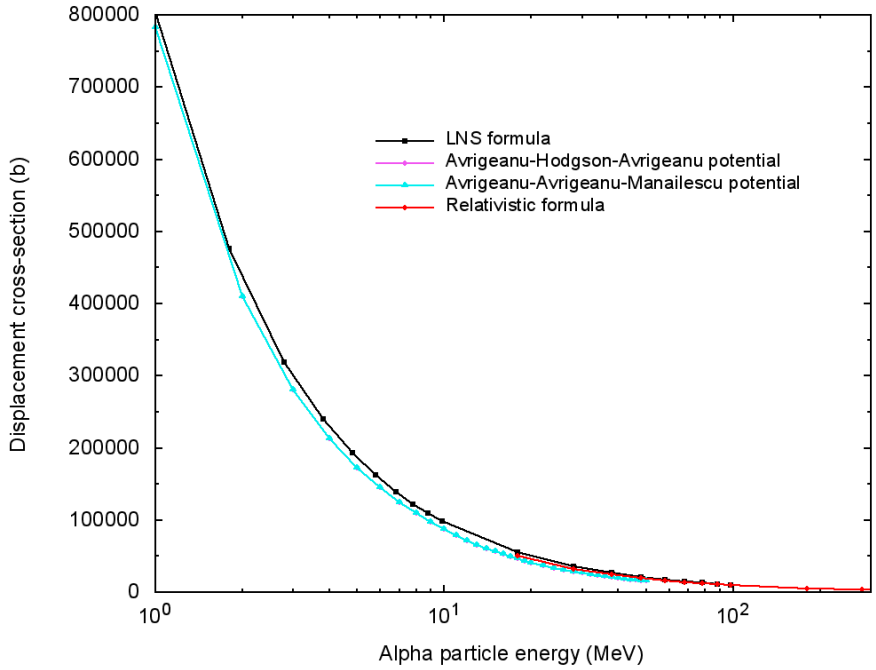

Fig. 2 Alpha-particle elastic displacement damage cross-section of Fe in different energy ranges. The curves using two different optical model potentials are almost overlapping.

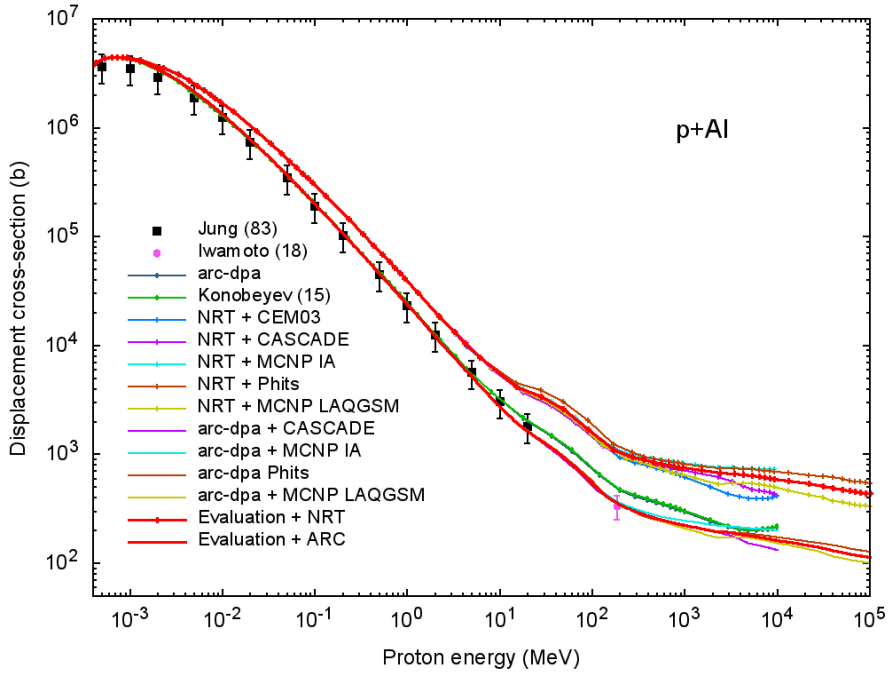

Fig. 3 Displacement damage cross-section for p+Al irradiation. All points are experimental data, which can be found in Table 3 and Jung's paper [54]; all lines and lines with dots are the calculated values. Arc-dpa, Konobeyev (15) and NRT + CEM03 are the proton displacement damage cross-sections calculated using arc-dpa model with original model parameters, arc-dpa coupling BCA model and NRT model, respectively, from Ref. [21]. Other results are calculated in this paper using four different nuclear models (CASCADE, INCL4.2 with ABLA, LAQGSM, PHITS's model) and two different displacement damage function models (arc-dpa model with new model parameters and NRT model).

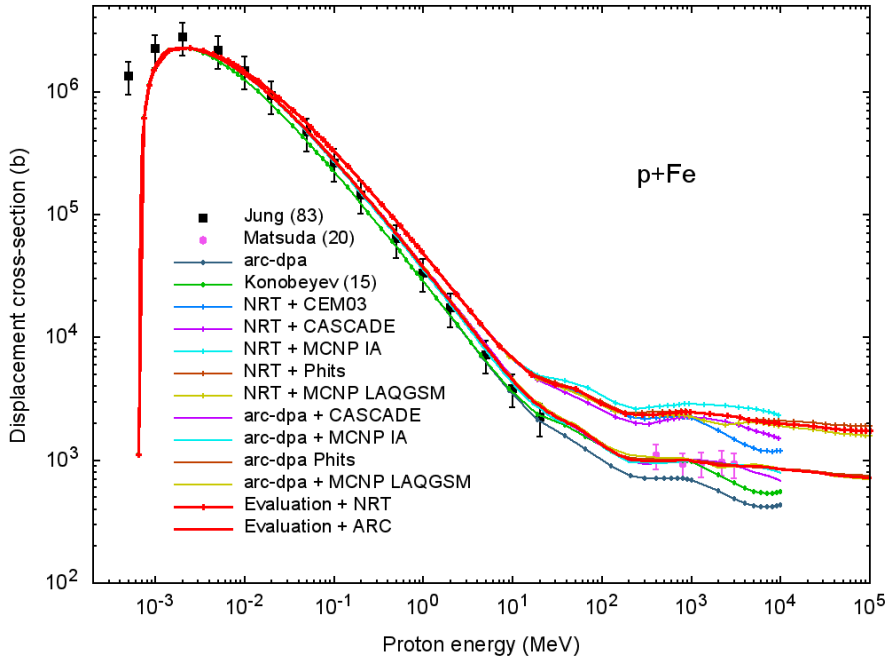

Fig. 4 The same as in Fig.3 for p+Fe irradiation

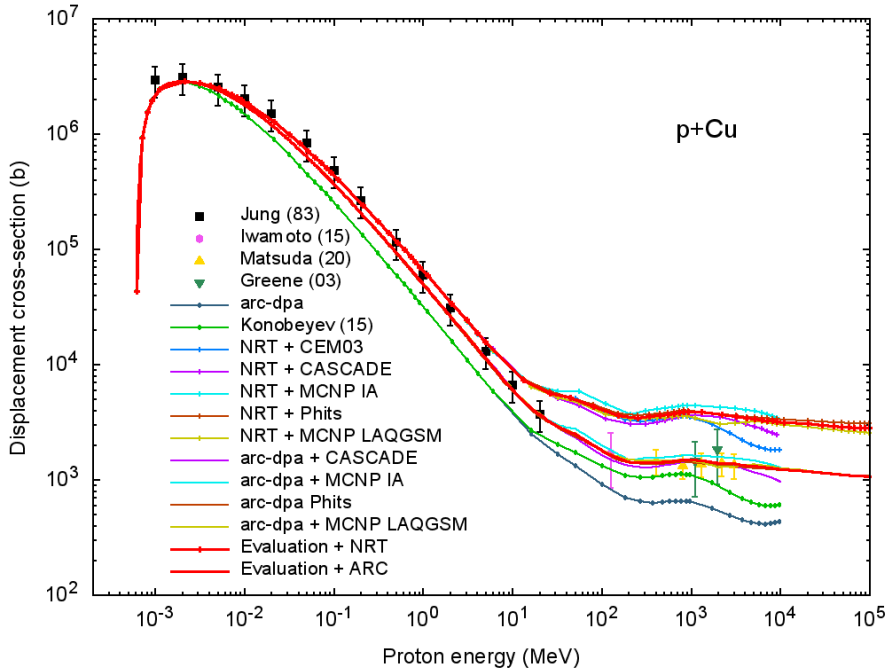

Fig. 5 The same as in Fig.3 for p+Cu irradiation

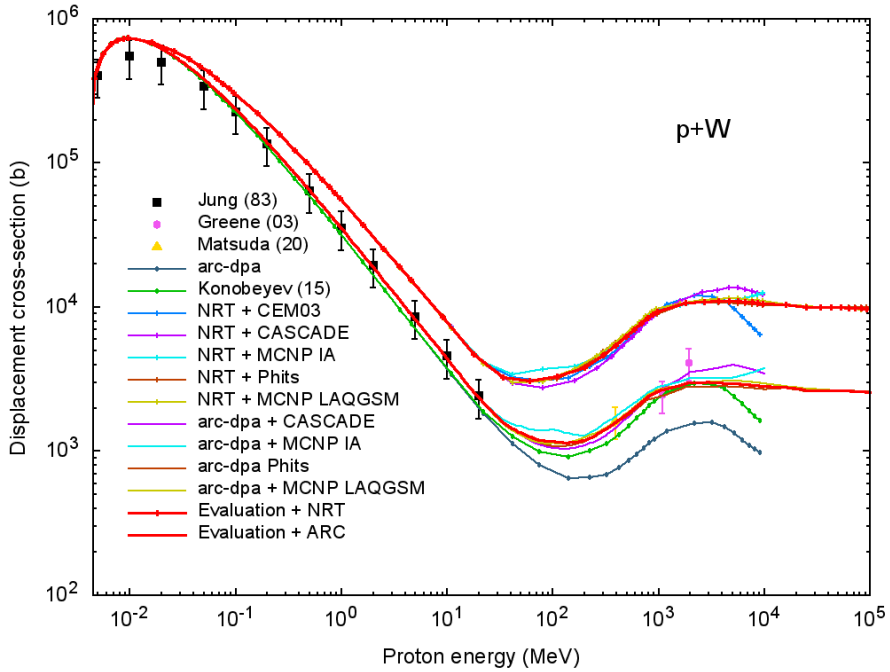

Fig. 6 The same as in Fig.3 for p+W irradiation

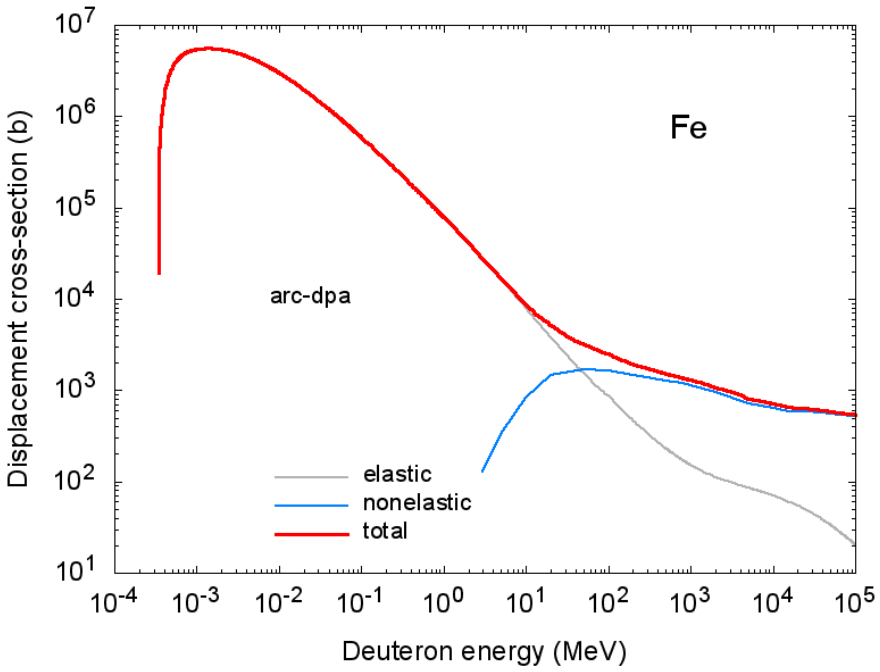

Fig. 7 The contribution of elastic scattering and nonelastic nuclear processes to the total displacement cross-section for d + Fe irradiation.

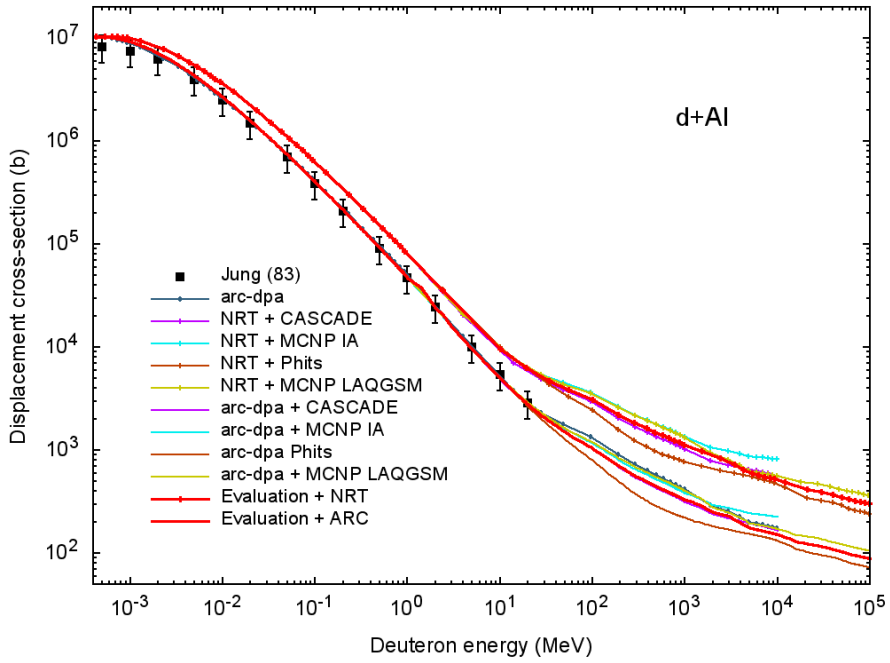

Fig. 8 Displacement damage cross-section for d+Al. The points are experimental data from Jung's paper [54]; all lines and lines with dots are the calculated values. Arc-dpa are the deuteron displacement damage cross-sections calculated using the arc-dpa model with original model parameters and the CASCADE model. Other results are calculated in this paper using four different nuclear models (CASCADE, INCL4.2 with ABLA, LAQGSM, PHITS's model) and two different displacement damage function models (arc-dpa model with new model parameters and NRT model).

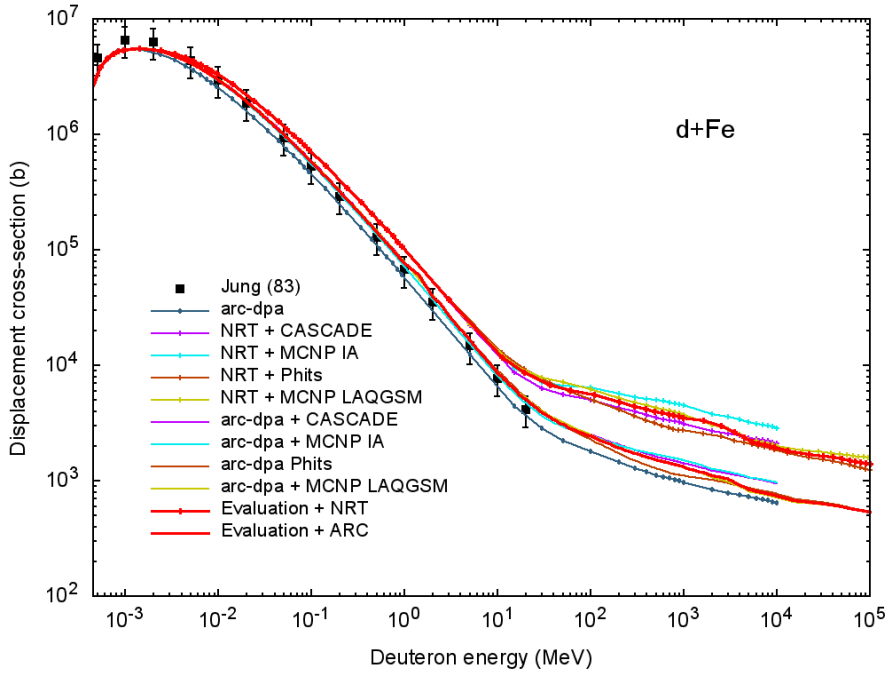

Fig. 9 The same as in Fig.8 for d+Fe irradiation

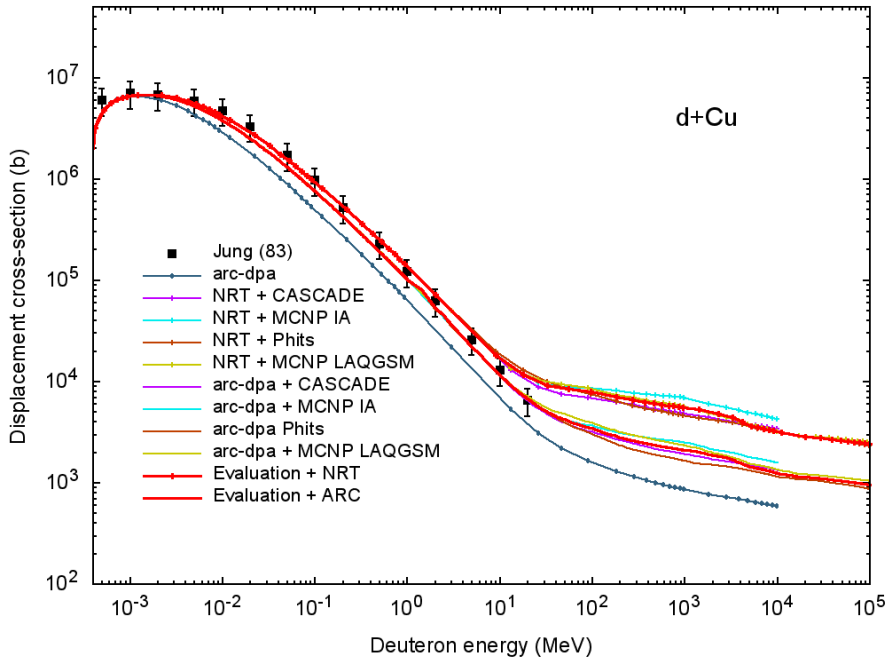

Fig. 10 The same as in Fig.8 for d+Cu irradiation

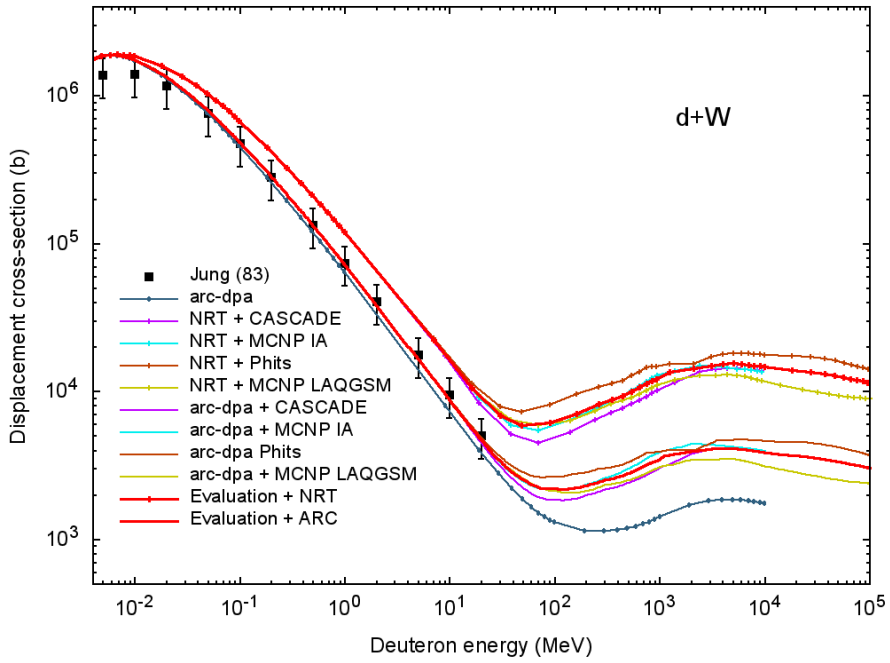

Fig. 11 The same as in Fig.8 for d+W irradiation

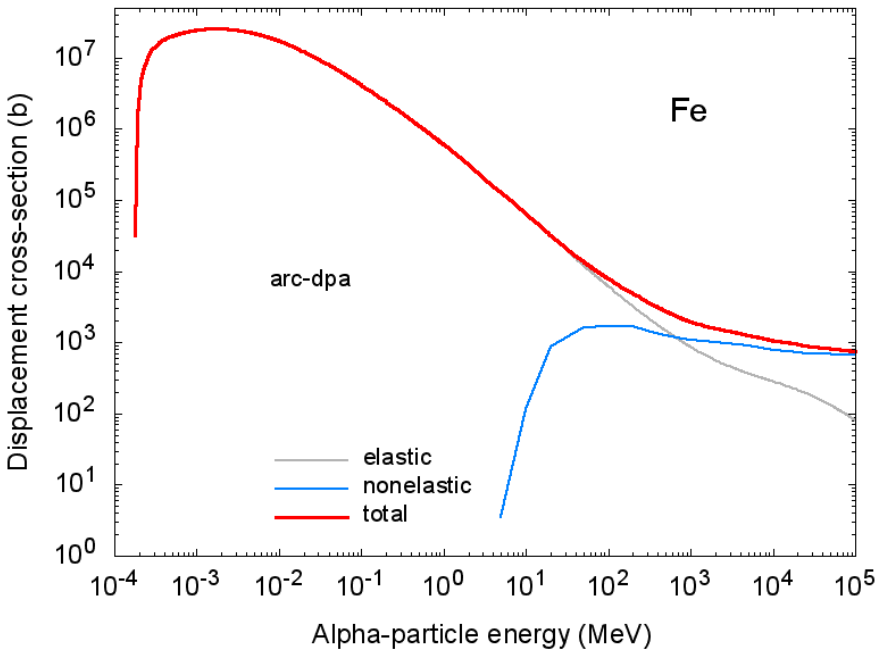

Fig. 12 The contribution of elastic scattering and nonelastic nuclear processes to the total displacement cross-section for α + Fe irradiation

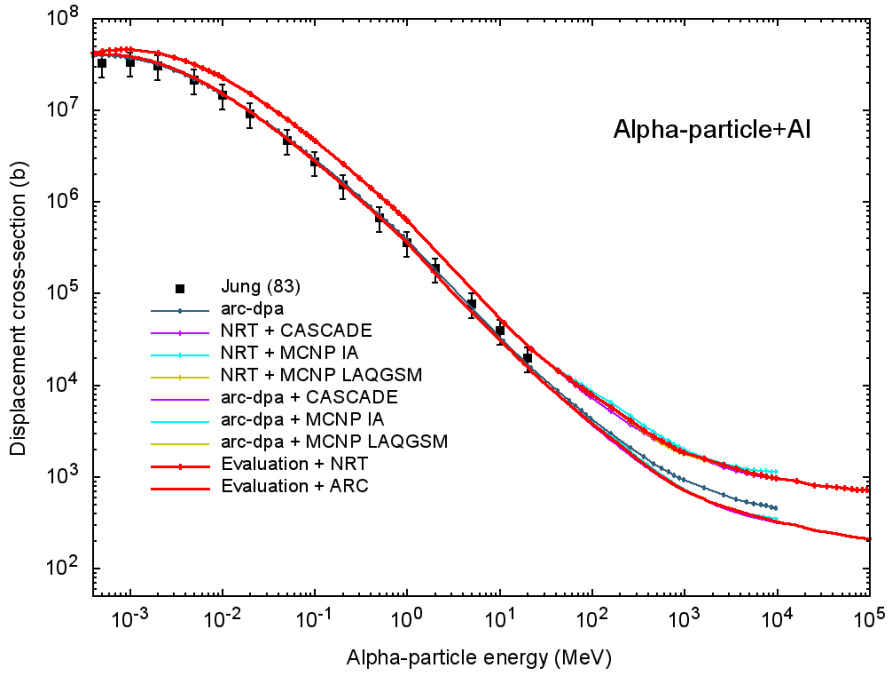

Fig. 13 Displacement damage cross-section for α+Al. The points are experimental data from Jung's paper [54]; all lines and lines with dots are the calculated values. Arc-dpa are the alpha-particle displacement damage cross-sections calculated using the arc-dpa model with original model parameters and the CASCADE model. Other results are calculated in this paper using four different nuclear models (CASCADE, INCL4.2 with ABLA, LAQGSM, PHITS's model) and two different displacement damage function models (arc-dpa model with new model parameters and NRT model).

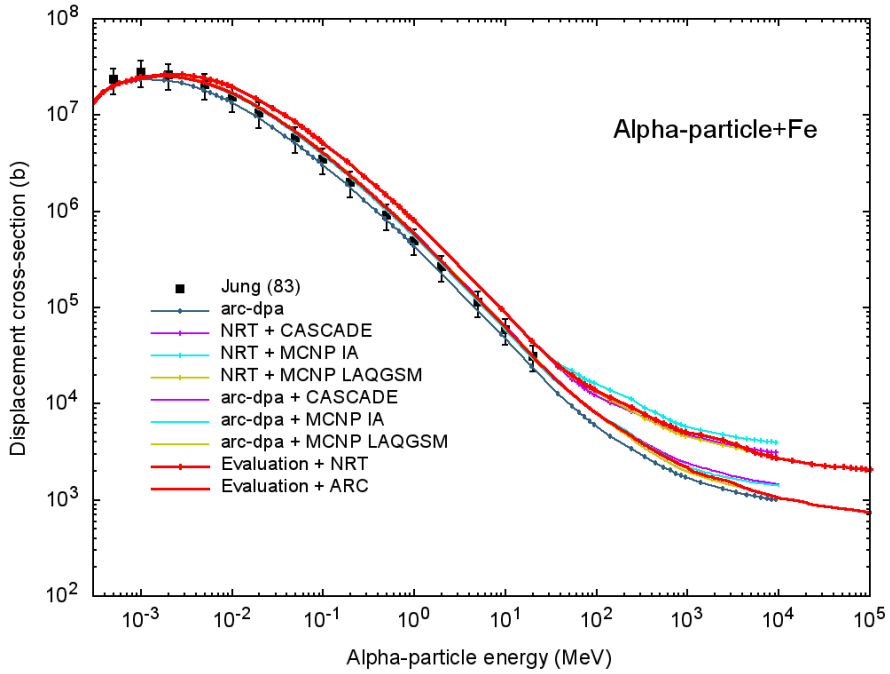

Fig. 14 The same as in Fig.13 for α+Fe irradiation

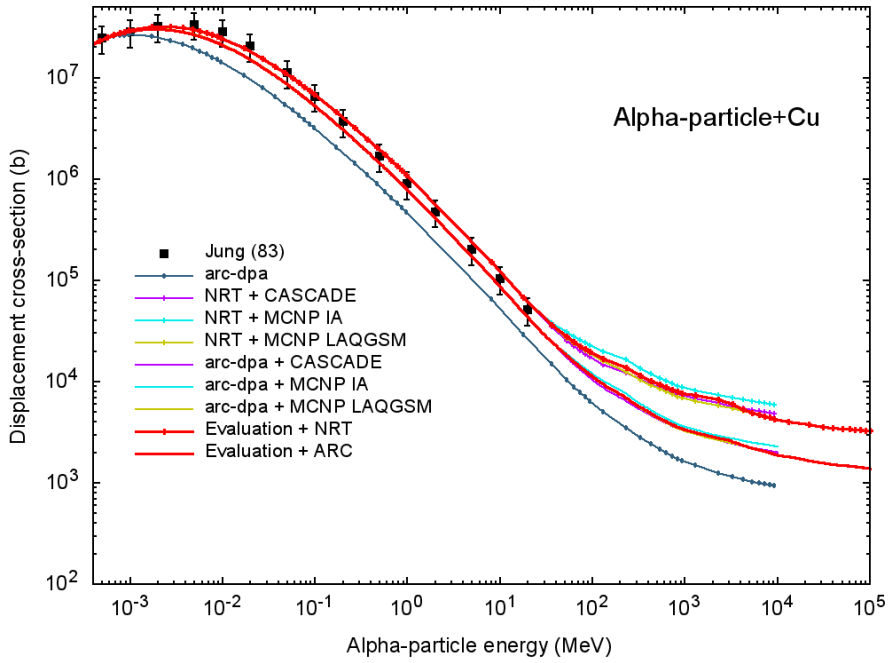

Fig. 15 The same as in Fig.13 for α+Cu irradiation

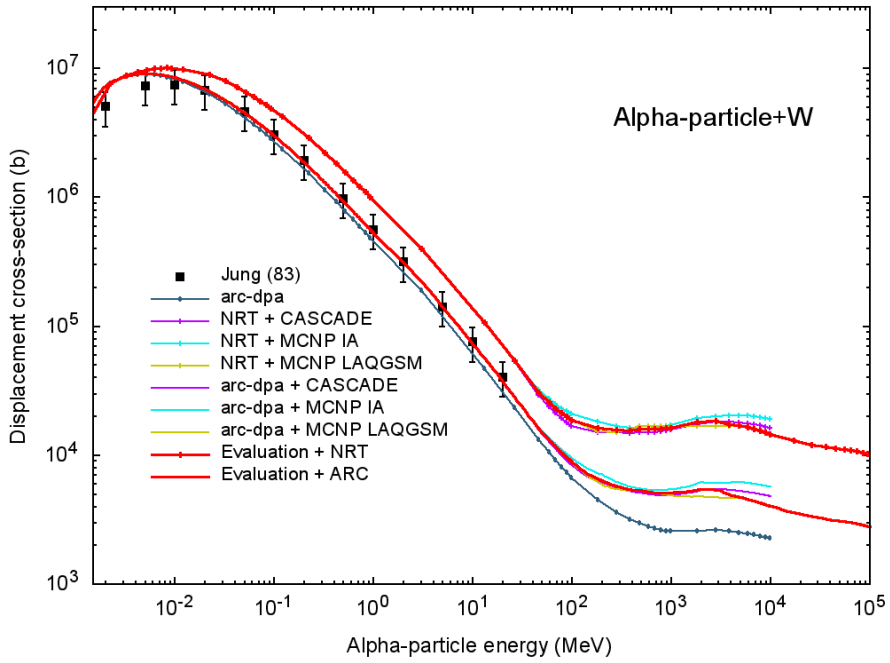

Fig. 16 The same as in Fig.13 for α+W irradiation

Table 1 Global optical model potentials for protons, deuterons and alpha-particles

Particle	Author	Energy Range	Z range	A range
p	Koning and and Delaroche [28]	0.001 – 200 MeV[a]	13 - 83[a]	27 – 209[a]
	Madland [29]	50 – 400 MeV[a]	6 - 82[a]	12 -208[a]
d	An and Cai [30]	1 – 200 MeV[a]	6 - 92[a]	12 - 238[a]
	Han, Shi and Shen [31]	1 – 200 MeV[a]	6 - 83[a]	12 - 209[a]
	Bojowald, Machner and Nann [32]	20 – 100 MeV[a]	6 - 82[a]	12 - 208[a]
α	Avrigeanu, Hodgson and Avrigeanu [33]	1 – 73 MeV[a]	8 - 96[a]	16 - 250[a]
	Avrigeanu, Avrigeanu and Mănăilescu [34]	1 - 50 MeV[b]	21 - 83	44 -209[b]

[a] : The data are taken from RIPL3 library [35];

[b] : The data are taken from Ref. [34].

Table 2 Overview of the codes dealing with nonelastic scattering interaction

Code	INC	Pre-equilibrium	Equilibrium	Projectiles	Upper energy limitation
MCNP6	Bertini	With	Dresner or ABLA	n, p	3.5 GeV
	ISABEL [40]	With	Dresner or ABLA	n, p d, t, ^{3}He, α	0.8 GeV 1 GeV/nucleon
	INCL4.2 [41]	Without	Dresner or ABLA	n, p, d, t, ^{3}He, α	~3 GeV/nucleon
	CEM03.03	With	GEM2	n, p	5 GeV (heavy nuclei-targets) 1 GeV (light nuclei-targets)
	LAQGSM03.03 [42]	With	GEM2	d, t, ^{3}He, α	1 TeV/nucleon
PHITS	INCL4.6	Without	GEM	n, p, d, t, ^{3}He, α	3 GeV/nucleon [a]
	JAM	Without	GEM	n, p	1 TeV
	JAMQMD	Without	GEM	d, t, ^{3}He, α	1 TeV/nucleon
CASCADE	Own model	Without	Own model	n, p, d, t, ^{3}He, α	~10 GeV

[a] : The JAM or JAMQMD models is used above 3 GeV/nucleon.

Table 3 Experimental proton displacement damage cross-section

Nuclide	Energy (GeV)	Damage rate (10^{-31} Ω m^3/proton)	Experiment	Displacement damage cross-section (b)
Al	0.185	1.3 [50]	RCNP	333
Fe	0.4	26.9 ± 0.7 [48]	J-PARC	1090 ± 253
	0.8	22.7 ± 0.4 [48]	J-PARC	925 ± 213
	1.3	23.2 ± 0.4 [48]	J-PARC	943 ± 218
	2.2	23.8 ± 0.3 [48]	J-PARC	969 ± 223
	3.0	22.8 ± 0.7 [48]	J-PARC	927 ± 218
Cu	0.125	3.41 [51]	KURRI	1550
	0.196	3.60 [50]	RCNP	1636
	1.1	3.66 [53]	AGS	1309
	1.94	2.88 [53]	AGS	1664
	0.4	3.21 ± 0.37 [48]	J-PARC	1460 ± 375
	0.8	2.93 ± 0.15 [48]	J-PARC	1330 ± 314
	1.3	3.03 ± 0.20 [48]	J-PARC	1380 ± 330
	2.2	3.07 ± 0.13 [48]	J-PARC	1390 ± 326
	3.0	2.97 ± 0.23 [48]	J-PARC	1350 ± 326
W	0.389	43.5 [49]	RCNP	1611
	1.1	65.9 [53]	AGS	2441
	1.94	110.5 [53]	AGS	4093

Table 4 New arc-dpa model parameters

Nuclide	Nuclear model	b	c
Al	CASCADE	-0.38	0.22
	INCL4.2 with ABLA (MCNP)	-0.36	0.20
	LAQGSM03.03 (MCNP)	-0.39	0.23
	PHITS's model	-0.28	0.09
Fe	CASCADE	-0.11	0.04
	INCL4.2 with ABLA (MCNP)	-0.17	0.10
	LAQGSM03.03(MCNP)	-0.11	0.03
	PHITS's model	-0.13	0.04
Cu	CASCADE	-0.12	0.03
	INCL4.2 with ABLA (MCNP)	-0.13	0.04
	LAQGSM03.03 (MCNP)	-0.11	0.01
	PHITS's model	-0.14	0.04
W	CASCADE	-0.60	0.28
	INCL4.2 with ABLA (MCNP)	-0.66	0.29
	LAQGSM03.03 (MCNP)	-0.57	0.26
	PHITS's model	-0.55	0.25